Available online at www.sciencedirect.com
SCIENCE DIRECT®
Journal of Organometallic Chemistry 690 (2005) 5159–5169
Journal of Organometallic Chemistry
www.elsevier.com/locate/jorganchem

Chiral molecular polygons based on the Pt-alkynyl linkage: Self-assembly, characterization, and functionalization

Hua Jiang, Wenbin Lin *

Department of Chemistry, CB#3290, University of North Carolina, Chapel Hill, NC 27599, USA

Received 7 February 2005; received in revised form 26 March 2005; accepted 28 March 2005
Available online 2 August 2005

Abstract

Treatment of 2,2′-diacetoxy-1,1′-binaphthyl-6,6′-bis(ethyne), **L**-H_2, with one equiv of *trans*-$Pt(PEt_3)_2Cl_2$ led to a mixture of different sizes of chiral metallocycles $[trans\text{-}(PEt_3)_2Pt(\mathbf{L})]_n$ (n = 3–8, **1**–**6**). Each of the chiral molecular polygons **1**–**6** was purified by silica-gel column chromatography and characterized by ^1H, $^{13}C\{^1H\}$, and $^{31}P\{^1H\}$ NMR spectroscopy, MS, IR, UV–Vis, and circular dichroism (CD) spectroscopies, size exclusion chromatography, and microanalysis. Chiral molecular square **2** was also characterized by single-crystal X-ray diffraction. The acetyl groups of **2** were readily deprotected under mild conditions to generate **2a** which possesses exposed chiral dihydroxy functional groups. The dihydroxy groups were functionalized with *n*-octadecyl chains or Fréchet-type dendrons to generate dendritic molecules built on a chiral molecular square core. This work shows the potential of generating interesting functional supramolecular systems based on Pt-alkynyl chiral molecular polygons.

Keywords: Chiral; Alkyne; Metallocycles; Platinum; Self-assembly; Supramolecular

1. Introduction

The self-assembly of supramolecular macrocyclic architectures has attracted intense interest in the past decade [1–7]. The synthesis of such polygonal structures typically utilizes appropriately designed rigid and directional building blocks, which can be classified into two types – linear and angular subunits. Each subunit has two active functional end groups to interact with other building blocks. With appropriate angular and linear building blocks, numerous small molecular polygons such as triangles and squares have been assembled [2–7]. Larger polygonal structures are, however, more scarce, as a direct consequence of their entropic disadvantage. Considering the equilibrium between a smaller cycle and a larger cycle, the enthalpy change is negligible ($\Delta H \sim 0$) when the steric effect and ring strains do not play a significant role. The free energy of the equilibrium between the two cyclic structures is dominated by the entropies of the cycles ($\Delta G = -T\Delta S$). Because more equivalents of the smaller cycle are needed to form the larger cycle, the entropy change is negative ($\Delta S < 0$) when the equilibrium is shifted to the larger cyclic structure. The free energy change in such an equilibrium shift is positive ($\Delta G > 0$) and therefore disfavored. Prior to our work, only a few molecular hexagons are known [8–15], and even fewer examples were reported for molecular pentagon [16], heptagon [17], and octagon [18].

In contrast to the above reversible reactions which produce the most thermodynamically stable products, irreversible reactions produce kinetically controlled products. In such cases, the self-correction mechanism is not operative. The design of building blocks with appropriate geometrical features is even more important for the successful synthesis of kinetically controlled

* Corresponding author. Tel.: +1 9199626320; fax: +1 9199622388.
E-mail address: wlin@unc.edu (W. Lin).

0022-328X/$ - see front matter © 2005 Published by Elsevier B.V.
doi:10.1016/j.jorganchem.2005.03.049

macrocycles. It is on the other hand possible to obtain larger cycles in a kinetically controlled reaction because different sizes of linear species can form, which will cyclize to give a mixture of different sizes of cycles. Smaller cycles are still typically favored over larger cycles in these reactions from kinetic considerations. Kinetically controlled macrocycle synthesis can be realized by forming covalent bonds or very strong metal–ligand bonds during the cyclization step [19–23]. The metal–alkynyl linkage provides a particularly useful building block for the construction of interesting supramolecular systems [24–27].

We are interested in the synthesis of chiral metallocycles using very strong metal–ligand coordination [28–32]. Well-defined enzyme-like chiral pockets or functionalities presented by these metallocycles can be utilized for enantioselective processes. Our recent work demonstrated the utility of chiral molecular triangles and squares in chiral sensing and asymmetric catalysis [28–30]. We have also recently demonstrated the synthesis of a highly electroluminescent chiral molecular square [31]. We wish to report in this article the one-pot self-assembly and extensive characterization of a family of chiral molecular polygons based on the robust Pt-alkynyl linkage, [*trans*-$(PEt_3)_2Pt(\mathbf{L})]_n$ (n = 3–8, **1–6**), by using *trans*-$Pt(PEt_3)_2$ group as the metal-connecting point and chiral 2,2′-diacetoxy-1,1′-binaphthyl-6,6′-bis(ethyne) as the bridging ligand [33].

2. Results and discussion

2.1. Self-assembly of chiral molecular polygons

The synthesis of ligand 2,2′-diacetoxy-1,1′-binaphthyl-6,6′-bis(ethyne) (**L**-H_2) was described previously [21]. As shown in Scheme 1, treatment of **L**-H_2 with one equiv of *trans*-$Pt(PEt_3)_2Cl_2$ in the presence of catalytic amounts of CuCl in CH_2Cl_2 and $HNEt_2$ at room temperature afforded a mixture of different sizes of chiral metallocycles [*trans*-$(PEt_3)_2Pt(\mathbf{L})]_n$ (n = 3–8, **1–6**). Each of the chiral molecular polygons was purified by silica-gel column chromatography, and analytically pure **1–6** was obtained in 5%, 18%, 16%, 10%, 5%, and 4% yield, respectively. The R_f values for these molecular polygons in hexane/ethyl acetate/CH_2Cl_2 (3:2:2 v/v/v) are 0.63, 0.47, 0.35, 0.31, 0.27, and 0.24, from the triangle to octagon, respectively. These results are in stark contrast with those of previously reported linear polymers which were synthesized under more forcing conditions [34].

2.2. Characterization of chiral molecular polygons

Compounds **1–6** have been characterized by $^1H\{^{31}P\}$, $^{13}C\{^1H\}$, and $^{31}P\{^1H\}$ NMR spectroscopy, FAB and MALDI-TOF MS, FT-IR, and microanalysis. The chiral molecular square **2** was also characterized by X-ray single crystal crystallography. Their optical properties, including UV–Vis and CD spectra, were studied as well.

$^1H\{^{31}P\}$ and $^{13}C\{^1H\}$ NMR spectra of metallocycles **1–6** indicated a single-ligand environment, consistent with the formation of cyclic species. As shown in Fig. 1, compounds **1–6** exhibit very similar $^1H\{^{31}P\}$ NMR spectra with the exception of two doublets around 7 ppm that are assigned to H7 and H8 on the naphthyl ring. The chemical shifts of H7 and H8 are sensitive to the dihedral angle between the naphthyl groups because of the influence of the ring current from the adjacent naphthyl group. The downfield shifts of the H7 and H8 signals observed from the triangle to hexagon indicate that the dihedral angle increases on going from the triangle to hexagon. In contrast, no downfield shifts were observed for the hexagon, heptagon, and octagon, suggesting that they exhibit adequate flexibility for the naphthyl groups to adopt similar dihedral angles. Downfield shifts were also observed for the C7 and C8 resonances for the triangle to hexagon in their $^{13}C\{^1H\}$ NMR spectra (Fig. 2). In $^{13}C\{^1H\}$ NMR spectra of molecular polygons, 10 carbon signals are observed between 150 and 120 ppm assignable to the binaphthyl groups. The peak at ~170 ppm is assigned to the acetoxy groups. The peaks between 109 and 110 ppm are assigned to the alkyne groups: the singlet with a set of satellite peaks ($^2J_{Pt-C} \approx 270$ Hz) is assigned to the alkyne carbon directly connected to the binaphathyl group while the triplet (due to coupling with *trans*-^{31}P, $^2J_{trans\text{-}P-C} \approx 14.5$ Hz) with a set of satellite peaks ($^1J_{Pt-C} \approx 970$ Hz) is assigned to the alkyne carbon directly connected to the Pt atom. The signal at ~20 ppm is assigned to the methyl group of the acetoxy group. The triplet at ~16.4 ppm (methylene) with coupling constant of $^1J_{P-C} = \sim 17$ Hz and the singlet at ~8.3 ppm (methyl) are assigned to the PEt_3 ligands. $^{31}P\{1H\}$ NMR spectra of **1–6** all exhibit a single peak at ~12.5 ppm with a set of satellite peaks ($^1J_{Pt-P} \approx$ 2366 Hz) (Fig. 3).

The FAB and MALDI-TOF MS data show molecular ion peaks M^+ or protonated peak $[M + H]^+$ for these chiral molecular polygons. Specifically, the FAB-MS data show M^+ = 2543.9 (Calcd. 2543.5) for the triangle, $[M + H]^+$ = 3392.4 (Calcd. 3392.3) for the square; M^+ = 4239.0 (Calcd. 4239.1) for the pentagon, and $[M + H]^+$ = 5088.2 (Calcd. 5087.9) for the hexagon. The MALDI-TOF-MS data show $[M + H]^+$ = 5939.2 (Calcd. 5935.7) for the heptagon and $[M + H]^+$ = 6787.1 (Calcd. 6782.5) for the octagon.

A single-crystal X-ray diffraction study on the molecular square **2** unambiguously demonstrated the formation of chiral molecular polygons (Fig. 4). Thin plate-shape X-ray diffraction-quality single crystals were obtained by slow evaporation of a solution of compound

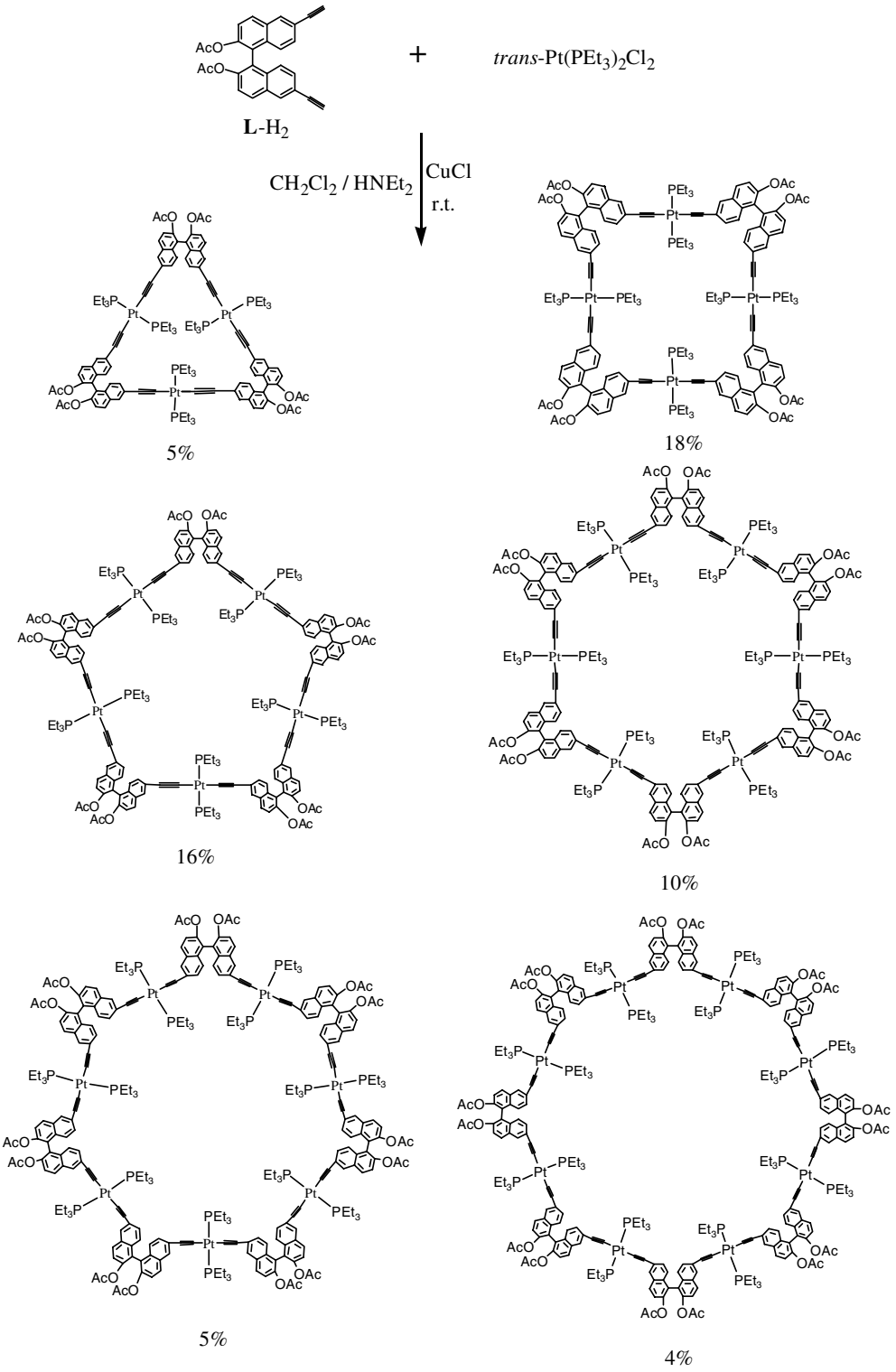

Scheme 1.

2 in dichloromethane and ethyl acetate. **2** crystallizes in the chiral monoclinic space group $P2_1$ (Table 1). The asymmetric unit of the crystal contains two molecules of [*trans*-$(PEt_3)_2Pt(\mathbf{L})]_4$, with the dihedral angles between the two naphthalene rings of 61.8°, 64.1°, 64.2°, 65.6°, 69.9°, 70.9°, 76.9°, and 77.0°, respectively. Selected bond distances and bond angles of **2** are listed in Table 2. The relatively large esd's in Table 2 are a result of poor quality of the single crystal. The simulated structures of other molecular polygons using Molecular Mechanics indi-

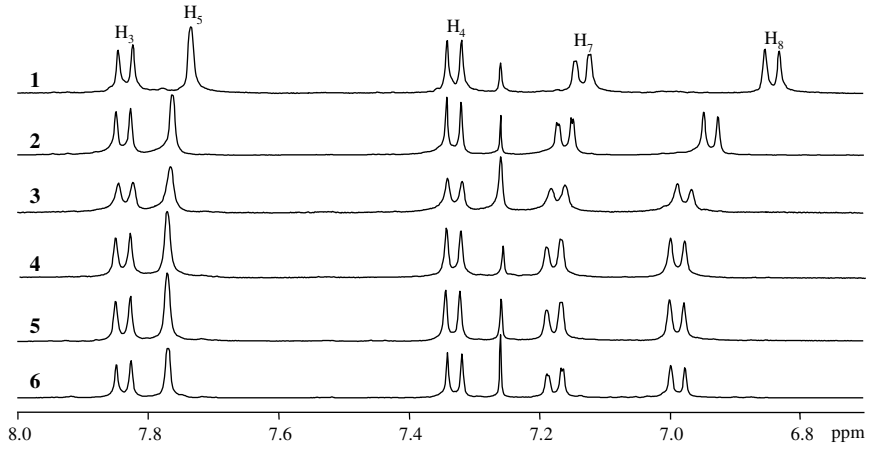

Fig. 1. $^{1}H\{^{31}P\}$ NMR spectra of molecular polygons **1**–**6**.

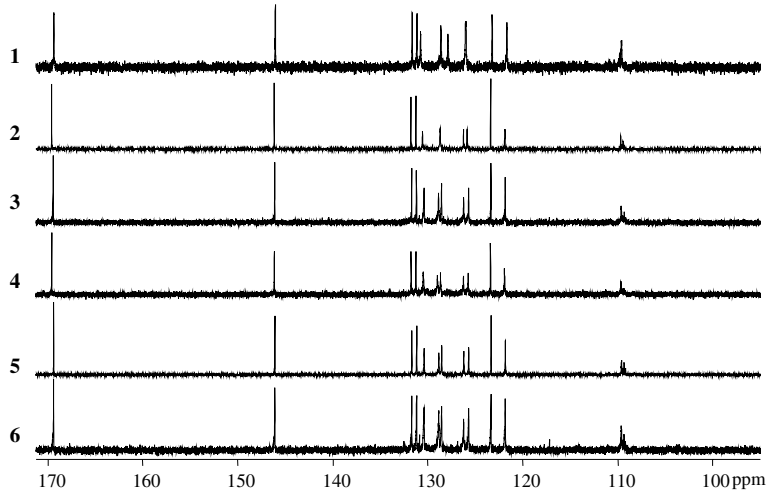

Fig. 2. $^{13}C\{^{1}H\}$ NMR spectra of molecular polygons **1**–**6**.

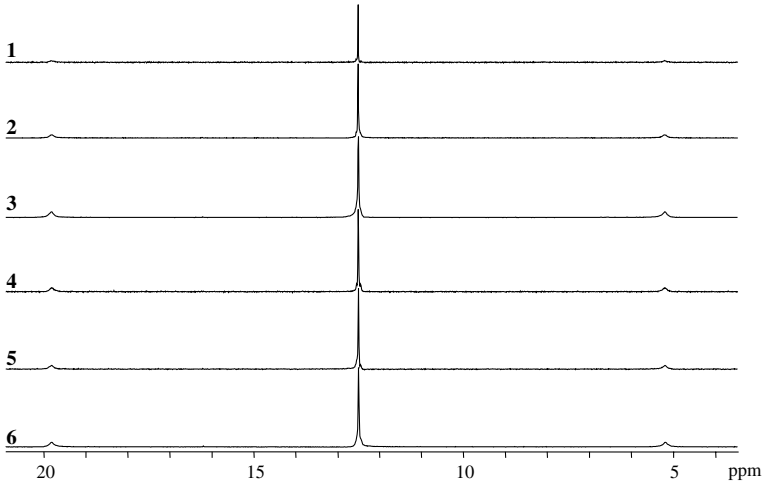

Fig. 3. $^{31}P\{^{1}H\}$ NMR spectra of molecular polygons **1**–**6**.

cated that **1**–**6** possess open cavities of 1.4–4.3 nm in size (Fig. 5). Consistent with the R_f values in silica-gel chromatography and Molecular Mechanics simulation results, the size exclusion chromatography (SEC) retention times for **1**–**6** are 30.81, 29.62, 28.72, 28.10, 27.53, and 27.08 min, respectively.

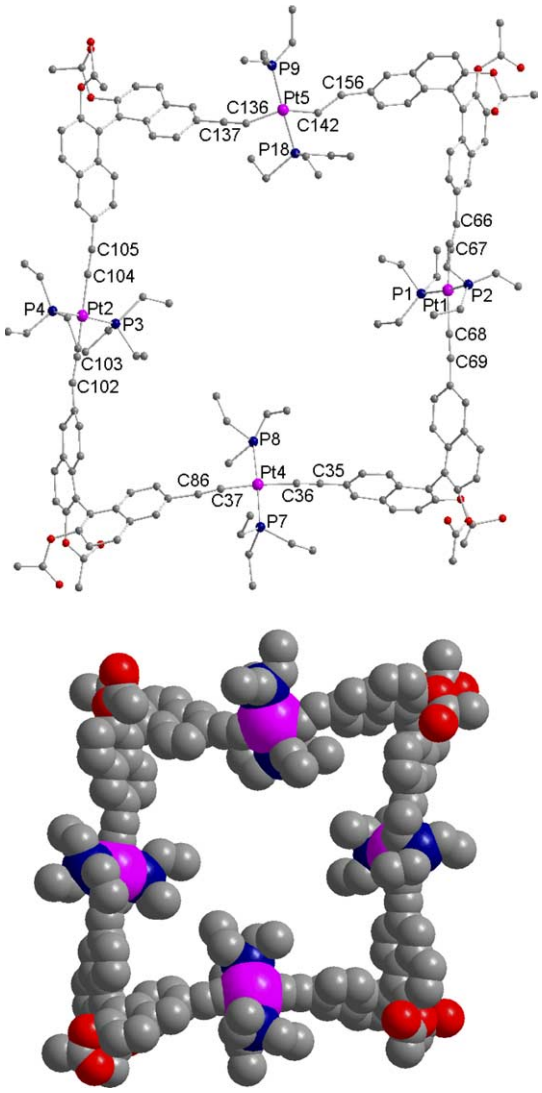

Fig. 4. Single-crystal X-ray structure (top) and a space-filling model (bottom) of molecular square **2**.

As expected, the terminal acetylenic C–H stretches of **L**-H_2 at ~3280 cm^{-1} disappeared upon the formation of metallocycles [*trans*-$(PEt_3)_2Pt(\mathbf{L})]_n$ (n = 3–8). The IR spectra of metallocycles exhibit expected C≡C stretches at ~2090 cm^{-1} (Fig. 6).

2.3. Optical properties of molecular polygons

The optical properties of **1**–**6** were studied by using UV–Vis and circular dichroism (CD) spectroscopies. The electronic spectrum of **L**-H_2 shows two peaks at 236 and 250 nm due to the naphthyl $\pi \rightarrow \pi^*$ transitions and a weak peak at 288 nm assignable to the acetylenic $\pi \rightarrow \pi^*$ transition. Upon the formation of metallocycles, a new intense peak at ~225 nm appeared, which can be assigned to the *trans*-$Pt(PEt_3)_2$ moiety (Fig. 7(a)). The acetylenic $\pi \rightarrow \pi^*$ transitions were significantly red-shifted and split into two peaks at 340 and 360 nm, a result of mixing of Pt p-orbitals into the acetylenic $\pi \rightarrow \pi^*$ bands [35]. Such bathochromic shifts for the acetylenic $\pi \rightarrow \pi^*$ transitions in these molecular polygons are much more pronounced than those observed in the metallocyclophanes built from [*cis*-$(PEt_3)_2PtCl_2$] and **L**-H_2 described previously [30]. This result is consistent with the more conjugated nature of **1**–**6** than previously reported metallocyclophanes. It is also interesting to note that the extinction coefficient increases as the size of the polygons increases, consistent with the presence of more *trans*-$Pt(PEt_3)_2$ and **L** building units in larger metallocycles.

CD spectra of metallocycles exhibit a bisignate band at ~260 nm due to the naphthyl $\pi \rightarrow \pi^*$ transition and two intense bands at ~350 and ~370 nm assignable to the acetylenic $\pi \rightarrow \pi^*$ transitions, along with a strong band at ~225 nm which can be attributed to the chiral arrangement of the PEt_3 groups on the Pt centers (Fig. 7(b)). Consistent with an increased number of *trans*-$Pt(PEt_3)_2$ and **L** building units, the CD signals also increase steadily as the size of the metallocycle increases.

2.4. Functionalization of chiral molecular square 2

The acetyl protecting groups in the metallocycles can be readily removed by treating [*trans*-$(PEt_3)_2Pt(\mathbf{L})]_n$ (**1**–**6**) with inorganic bases to give hydroxyl-containing metallocycles [*trans*-$(PEt_3)_2Pt(\mathbf{L}_1)]_n$ ($\mathbf{L}_1$-H_2 is 2,2′-dihydroxy-1,1′-binaphthyl-6,6′-bis(ethyne)). Specifically, the molecular square [*trans*-$(PEt_3)_2Pt(\mathbf{L})]_4$ was treated with K_2CO_3 in a mixture of MeOH and THF to afford metallocycle [*trans*-$(PEt_3)_2Pt(\mathbf{L}_1)]_4$ (**2a**) with the hydroxy functional groups. Such hydroxyl-containing metallocycles provide a platform for the synthesis of metallocycles with different functionalities. For example, treatment of **2a** with excess 1-bromooctadecane afforded molecular square with *n*-octadecyl protecting groups, **2b**, in 50% isolated yield. Treatment of **2a** with excess Fréchet type of dendron G_1Br afforded molecular square with dendron G_1 protecting groups, **2c**, in 43% isolated yield (Scheme 2).

All of the molecular squares, **2a**, **2b**, and **2c**, were characterized by $^1H\{^{31}P\}$, $^{31}P\{^1H\}$ NMR, SEC, and MALDI-TOF MS spectroscopy. The $^1H\{^{31}P\}$, $^{31}P\{^1H\}$, and $^{13}C\{^1H\}$ NMR spectra of **2a** show a single-ligand environment with similar peaks to the acetyl-protected square **2** with the exception of the missing acetyl groups and the presence of a new peak for the –OH group. The $^1H\{^{31}P\}$ and $^{31}P\{^1H\}$ NMR spectra of **2b** and **2c** are consistent with a single-ligand environment. The MALDI-TOF MS spectra show ionized peaks ($[M + H]^+$, $[M + Na]^+$, and $[M + K]^+$) for **2a**, **2b**, and **2c**.

Table 1
Crystal data of **2**

Chemical formula	$C_{160}H_{368}O_{32}P_{16}Pt_8$[a]
Crystal system	Monoclinic
a (Å)	25.19(6)
b (Å)	25.96(7)
c (Å)	27.35(9)
β (°)	106.65(14)
V (Å^3)	17138(81)
Z	2
Formula weight	6782.38
Space group	$P2_1$
T (K)	173(2)
λ(Mo Kα) (Å)	0.71073
ρ_{calc} (g/cm^3)	1.314
μ(Mo Kα) (cm^{-1})	33.83
Number of observed reflections ($I > 2\sigma(I)$)	15683
Number of parameters	1585
Minimum and maximum residual density (e/Å^3)	5.083[b] and −1.457
R_1	0.1252
wR_2	0.2547
Goodness-of-fit	1.056
Flack parameter	0.021(14)

[a] Two molecules in the asymmetric unit.
[b] The residual electron density is located near Pt centers.

Table 2
Selected bond distances (Å) and bond angles (°) for **2**

Bond lengths (Å)		Bond angles (°)	
Pt(1)–C(67)	2.03(5)	C(67)–Pt(1)–C(68)	173(2)
Pt(1)–C(68)	2.14(6)	C(67)–Pt(1)–P(2)	92(2)
Pt(1)–P(2)	2.23(2)	C(68)–Pt(1)–P(2)	89(2)
Pt(1)–P(1)	2.27(2)	C(67)–Pt(1)–P(1)	88(2)
Pt(2)–C(103)	1.98(4)	C(68)–Pt(1)–P(1)	93(2)
Pt(2)–C(104)	2.04(4)	P(2)–Pt(1)–P(1)	170.2(6)
Pt(2)–P(4)	2.27(2)	C(103)–Pt(2)–C(104)	179(2)
Pt(2)–P(3)	2.27(2)	C(103)–Pt(2)–P(4)	90(2)
Pt(3)–C(208)	1.99(4)	C(104)–Pt(2)–P(4)	91(2)
Pt(3)–C(226)	1.97(5)	C(103)–Pt(2)–P(3)	87(2)
Pt(3)–P(5)	2.31(2)	C(104)–Pt(2)–P(3)	93(2)
Pt(3)–P(10)	2.32(2)	P(4)–Pt(2)–P(3)	172.3(6)
Pt(4)–C(37)	1.93(3)	C(208)–Pt(3)–C(226)	174(2)
Pt(4)–C(36)	2.01(5)	C(208)–Pt(3)–P(5)	85(2)
Pt(4)–P(7)	2.28(2)	C(226)–Pt(3)–P(5)	93(2)
Pt(4)–P(8)	2.30(2)	C(208)–Pt(3)–P(10)	93(2)
Pt(5)–C(136)	2.07(6)	C(226)–Pt(3)–P(10)	89(2)
Pt(5)–C(142)	2.08(2)	P(5)–Pt(3)–P(10)	177.5(5)
Pt(5)–P(18)	2.27(2)	C(37)–Pt(4)–C(36)	172(2)
Pt(5)–P(9)	2.34(2)	C(37)–Pt(4)–P(7)	87(2)
Pt(6)–C(292)	1.97(6)	C(36)–Pt(4)–P(7)	91(2)
Pt(6)–C(220)	1.94(7)	C(37)–Pt(4)–P(8)	90(2)
Pt(6)–P(13)	2.19(2)	C(36)–Pt(4)–P(8)	92(2)
Pt(6)–P(15)	2.33(2)	P(7)–Pt(4)–P(8)	177.4(5)
Pt(7)–C(321)	2.03(8)	C(136)–Pt(5)–C(142)	144(2)
Pt(7)–C(77)	2.11(6)	C(136)–Pt(5)–P(18)	82(2)
Pt(7)–P(11)	2.28(2)	C(142)–Pt(5)–P(18)	64(4)
Pt(7)–P(12)	2.31(2)	C(136)–Pt(5)–P(9)	97(2)
Pt(8)–P(16)	2.19(2)	C(142)–Pt(5)–P(9)	114(4)
Pt(8)–C(252)	1.81(7)	P(18)–Pt(5)–P(9)	178.9(7)
Pt(8)–C(307)	2.24(7)	C(292)–Pt(6)–C(220)	171(3)
Pt(8)–P(17)	2.38(2)	C(292)–Pt(6)–P(13)	85(2)
C(76)–C(77)	1.25(6)	C(220)–Pt(6)–P(13)	97(2)
C(35)–C(36)	1.27(6)	C(292)–Pt(6)–P(15)	88(2)
C(37)–C(86)	1.20(5)	C(220)–Pt(6)–P(15)	92(2)
C(66)–C(67)	1.29(5)	P(13)–Pt(6)–P(15)	167(2)
C(68)–C(69)	1.15(6)	C(321)–Pt(7)–C(77)	173(3)
C(102)–C(103)	1.30(5)	C(321)–Pt(7)–P(11)	89(2)
C(104)–C(105)	1.24(5)	C(77)–Pt(7)–P(11)	92(2)
C(136)–C(137)	1.24(6)	C(321)–Pt(7)–P(12)	93(2)
C(142)–C(156)	1.63(8)	C(77)–Pt(7)–P(12)	86(2)
C(208)–C(209)	1.22(5)	P(11)–Pt(7)–P(12)	177.7(8)
C(220)–C(221)	1.33(7)	P(16)–Pt(8)–C(252)	79(2)
C(225)–C(226)	1.26(6)	P(16)–Pt(8)–C(307)	89(2)
C(251)–C(252)	1.44(6)	C(252)–Pt(8)–C(307)	168(2)
C(292)–C(293)	1.22(8)	P(16)–Pt(8)–P(17)	175.2(8)
C(171)–C(321)	1.29(7)	C(252)–Pt(8)–P(17)	100(2)
C(239)–C(307)	1.09(8)	C(307)–Pt(8)–P(17)	92(2)

The retention time of **2a** in SEC is 31.62 min, which is longer than that of **2** (29.62 min). This is consistent with the smaller size of **2a** in comparison to **2**. In fact, based on SEC retention times, **2a** appears even smaller than **1** (retention time of 30.81 min), indicating that the acetyl groups contribute significantly to the overall size of the metallocycles because these acetyl groups are located outside of the metallocycles. The retention time of **2b** is 27.98 min, which is between the retention times of hexagon **4** (28.10 min) and heptagon **5** (27.53 min) with the acetyl protecting groups. The retention time of **2c** is 27.34 min, which is between the retention times of heptagon **5** (27.53 min) and octagon **6** (27.08 min) with acetyl protecting groups.

3. Summary

We have successfully demonstrated the facile self-assembly of molecular polygons from the triangle to octagon. They are well characterized by $^1H\{^{31}P\}$, $^{13}C\{^1H\}$, and $^{31}P\{^1H\}$ NMR spectroscopy, FAB and MALDI-TOF MS, FT-IR, and microanalysis. Their optical properties, including UV–Vis and CD, were studied. We believe that limited conformational flexibility of the bridging ligand is key to the facile one-pot self-assembly of chiral molecular polygons **1**–**6**. This work represents a rare example in which multiple products can be readily isolated from a coordination-directed self-assembly process. Further functionalization of these metallocycles with *n*-octadecyl and Fréchet-type dendrons were also achieved. Tunable cavities and chiral functionalities presented by these molecular polygons promise to make them excellent receptors for a variety of guests.

4. Experimental

4.1. Materials and general procedures

All of the chemicals were obtained from commercial sources and used without further purification. All of the reactions and manipulations were carried out under

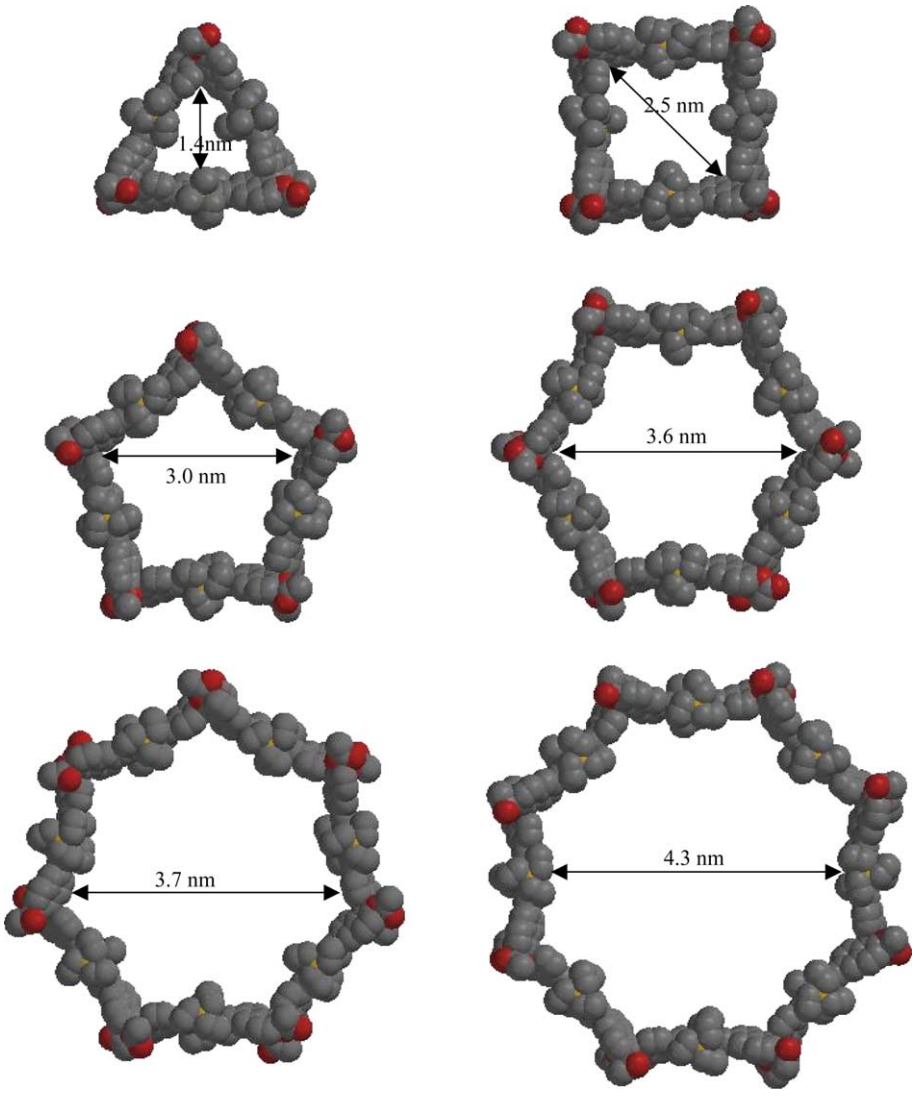

Fig. 5. Space filling models of energy minimized structures of molecular polygons **1**–**6**.

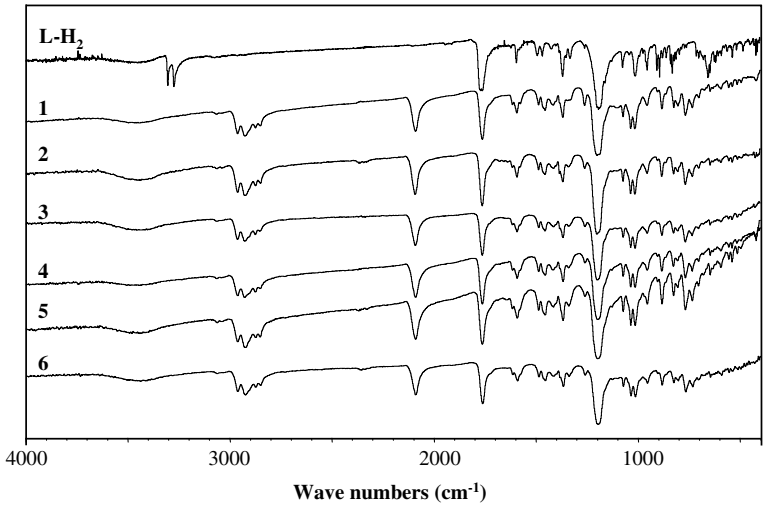

Fig. 6. FT-IR spectra of metallocycles **1**–**6**.

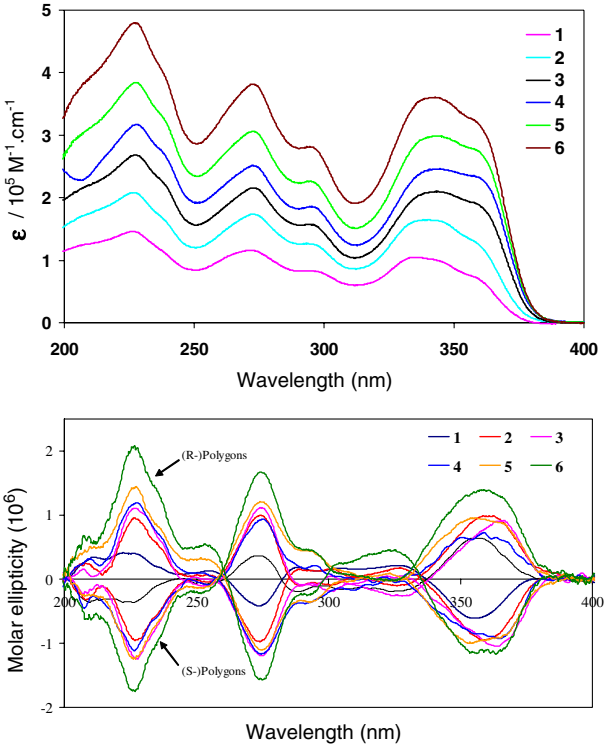

Fig. 7. UV–Vis (top) and CD spectra (bottom) of metallocycles **1**–**6**.

N_2 with the use of standard inert atmosphere and Schlenk techniques. Solvents used in reactions were dried by standard procedures. *trans*-[$Pt(PEt_3)_2Cl_2$] was prepared according to the literature procedures [36]. The IR spectra were recorded from KBr pellets on a Nicolet Magna-560 FT-IR spectrometer. NMR spectra were recorded on Bruker NMR 400 DRX spectrometer. ^1H NMR spectra were recorded at 400 MHz and referenced to the proton resonance resulting from incomplete deuteration of the deuterated chloroform (δ 7.26). $^{13}C\{^1H\}$ NMR spectra were recorded at 100 MHz, and all of the chemical shifts are reported downfield in ppm relative to the carbon resonance of chloroform-d_1 (δ 77.0).

The energy minimizations were performed based on Molecular Mechanics for Equilibrium Geometry Optimization using AM1 in the PC-Spartan package. FAB-MS spectra were taken at Mass Spectrometry Facility at Michigan State University, while MALDI-TOF mass spectra were taken at Mass Spectrometry Lab at University of Illinois at Urbana-Champaign.

4.2. Optical measurements (UV–Vis and CD)

UV–Vis spectra were obtained using Shimadzu UV-2410PC spectrophotometer. CD spectra were recorded on a Jasco J-720 spectropolarimeter. Conditions: metallocycles were dissolved in acetonitrile with concentrations in the order of 10^6–10^5 M. Due to the poor solubility of larger metallocycles in acetonitrile, they were dissolved in acetonitrile with the addition of varying amounts of dichloromethane. The measurements were carried out in 1 mm cell. Triangle, square, and pentagon were dissolved in acetonitrile. Hexagon, heptagon, and octagon were dissolved in acetonitrile with 0.8% dichloromethane.

4.3. Size exclusion chromatography

SEC was performed on an HPLC using PLgel columns (Polymer Laboratories, 5 μm, 7.5 × 300 mm) of 10^3 Å pore size. Conditions: mobile phase = dichloromethane (Aldrich, Certified A.C.S.), flow rate = 0.25 mL/min, injection volume = 10 μL. Sample detection was achieved by absorption spectroscopy using a diode array detector at 300 nm (±10 nm band width). Polystyrene standards (M_w;= 2500, 13 000, 30 000, and 50 000) were purchased from Aldrich. Polystyrene was detected at a wavelength of 254 nm.

The determination of the unit cells and data collection for compound **2** were performed on a Siemens SMART 1000 CCD diffractometer. The data were collected using graphite-monochromatic Mo Kα radiation (λ = 0.71073 Å) at 173 K. The data sets were corrected by SADABS program. The structure was solved by direct methods, and refined by full-matrix least-squares methods with the SHELXTL-97 program package.

4.4. Synthesis of (*R*)-[*trans*-$(PEt_3)_2Pt(L)]_n$ (***n*** = 3–8, ***1***–***6***)

To a solution of (*R*)-**L**-H_2 (209 mg, 0.5 mmol) and *trans*-$Pt(PEt_3)_2Cl_2$ (250 mg, 0.5 mmol) in deareated dichloromethane (200 mL) and diethylamine (1 mL), was added CuCl (10 mg, 0.1 mmol). After being stirred at room temperature for 50 min, the reaction mixture was washed with water three times. The organic layer was dried over anhydrous $MgSO_4$ and the organic volatiles were removed in vacuum. The residue was purified by silica-gel column chromatography with an eluent of hexane/ethyl acetate/dichloromethane (from 3:1:1 v/v/v to 2:1:1 v/v/v) to afford (*R*)-[*trans*-$(PEt_3)_2Pt$(**L**)]$_n$ (n = 3–8, **1**–**6**) as the light yellow solids. The isolated yields are: **1** (21 mg, 5%), **2** (77 mg, 18%), **3** (68 mg, 16%), **4** (43 mg, 10%),**5** (21 mg, 5%), and **6** (18 mg, 4%). The R_f values for compounds **1**–**6** in thin layer chromatography plates using an eluent of hexane/ethyl acetate/CH_2Cl_2 (3:2:2, v/v/v) are: n = 3, 0.628; n = 4, 0.465; n = 5, 0.352; n = 6, 0.310; n = 7, 0.268; n = 8, 0.239.

4.4.1. (*R*)-[*trans*-$(PEt_3)_2Pt(L)]_3$ (***1***)

$^1H\{^{31}P\}$ NMR ($CDCl_3$): δ 7.83 (d, ^3J = 8.8 Hz, 6H), 7.73 (s, 6H), 7.33 (d, ^3J = 8.8 Hz, 6H), 7.13 (dd,

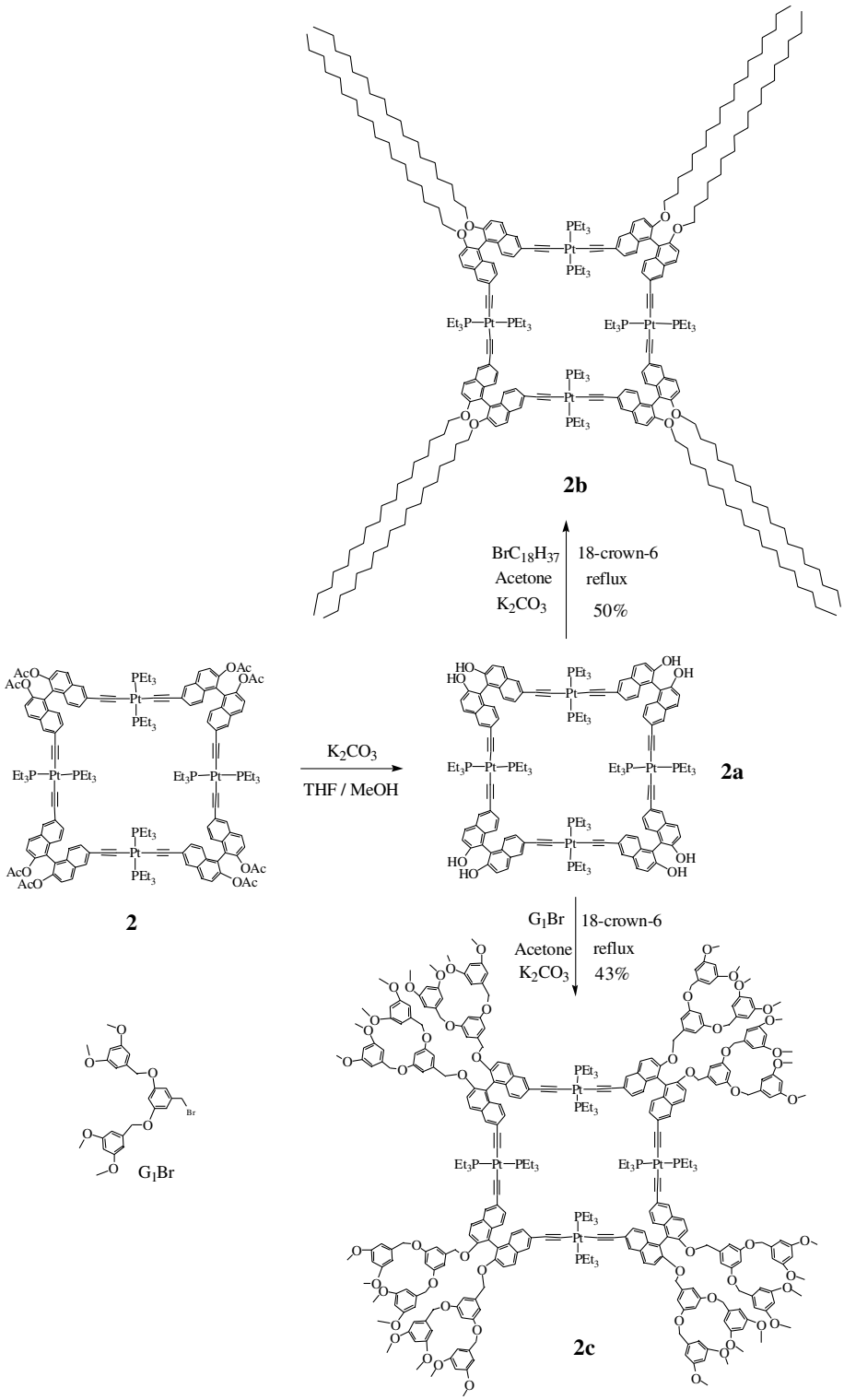

Scheme 2.

^{3}J = 8.8 Hz, ^{4}J = 1.47 Hz, 6H), 6.84 (d, ^{3}J = 8.8 Hz, 6H), 2.16 (m, 36H), 1.96 (s, 18H), 1.20 (t, ^{3}J = 7.3 Hz, 54H). $^{31}P\{^{1}H\}$ NMR ($CDCl_3$): δ 12.60 ($^{1}J_{P-Pt}$ = 2363.2 Hz). $^{13}C\{^{1}H\}$ NMR ($CDCl_3$): δ 169.4, 146.0, 131.6, 131.1, 130.7, 128.6, 127.8, 125.99, 125.95, 123.2, 121.6, 109.7 (t, $^{1}J_{Pt-C}$ = 983.5 Hz, $^{2}J_{P-C}$ = 15.2 Hz), 109.6 (s, $^{2}J_{Pt-C}$ = 271.2 Hz), 20.6, 16.2 (t, $^{1}J_{P-C}$ = 17.6 Hz), 8.26. IR: ν(–C≡C–) 2090.1 cm^{-1} (m), ν (–C=O) 1762.1 cm^{-1} (s); MS (FAB): *m*/*z* 2543.9 (Calcd. *m*/*z* 2543.5 for M^{+}). Anal. Calc. for $C_{121}H_{140}Cl_2O_{12}P_6$-

$Pt_3 \cdot CH_2Cl_2$: C, 55.3; H, 5.37; N, 0.0. Found: C, 55.0; H, 4.88; N, 0.29%.

*4.4.2. (R)-[trans-$(PEt_3)_2Pt(\mathbf{L})$]$_4$ (**2**)*

$^1H\{^{31}P\}$ NMR ($CDCl_3$): δ 7.84 (d, ^3J = 8.8 Hz, 8H), 7.77 (s, 8H), 7.33 (d, ^3J = 8.8 Hz, 8H), 7.16 (d, ^3J = 8.8 Hz, 8H), 6.94 (d, ^3J = 8.8 Hz, 8H), 2.18 (m, 48H), 1.91 (s, 24H), 1.22 (t, ^3J = 7.3 Hz, 72H). $^{31}P\{^1H\}$ NMR ($CDCl_3$): δ 12.50 ($^1J_{P-Pt}$ = 2366.3 Hz). $^{13}C\{^1H\}$ NMR ($CDCl_3$): δ 169.5, 146.0, 131.6, 131.1, 130.4, 128.61, 128.56, 126.1, 125.7, 123.3, 121.8, 109.6 (s, $^2J_{Pt-C}$ = 270.4 Hz), 109.31 (t, $^1J_{Pt-C}$ = 975.1 Hz, $^2J_{P-C}$ = 14.8 Hz), 20.6, 16.3 (t, $^1J_{P-C}$ = 17.6 Hz), 8.32. IR: ν(–C≡C–) 2091.8 cm^{-1} (m); ν(–C=O) 1762.7 cm^{-1} (s); MS (FAB): *m/z* 3392.4 (Calcd. *m/z* 3392.3 for $[M + H]^+$). Anal. Calc. for $C_{160}H_{184}O_{16}P_8Pt_4$: C, 56.7; H, 5.47; N, 0.0. Found: C, 57.0; H, 5.66; N, 0.55%.

*4.4.3. (R)-[trans-$(PEt_3)_2Pt(\mathbf{L})$]$_5$ (**3**)*

$^1H\{^{31}P\}$ NMR ($CDCl_3$): δ 7.85 (d, ^3J = 8.8 Hz, 10H), 7.78 (s, 10H), 7.34 (d, ^3J = 8.8 Hz, 10H), 7.19 (d, ^3J = 8.8 Hz, 10H), 6.99 (d, ^3J = 8.8 Hz, 10H), 2.19 (m, 60H), 1.88 (s, 30H), 1.23 (t, ^3J = 7.3 Hz, 90H). $^{31}P\{^1H\}$ NMR ($CDCl_3$): δ 12.45 ($^1J_{P-Pt}$ = 2368.1 Hz). $^{13}C\{^1H\}$ NMR ($CDCl_3$): δ 169.4, 146.1, 131.7, 131.1, 130.4, 128.8, 128.5, 126.2, 125.7, 123.3, 121.8, 109.6 (s, $^2J_{Pt-C}$ = 269.8 Hz), 109.26 (t, $^1J_{Pt-C}$ = 969.5 Hz, $^2J_{P-C}$ = 14.6 Hz), 20.6, 16.4 (t, $^1J_{P-C}$ = 17.6 Hz), 8.34. IR: ν(–C≡C–) 2090.6 cm^{-1} (m); ν(–C=O) 1762.4 cm^{-1} (s). MS (FAB): *m/z* 4239.0 (Calcd. *m/z* 4239.1 for M^+). Anal. Calc. for $C_{201}H_{232}Cl_2O_{20}P_{10}Pt_5 \cdot CH_2Cl_2$: C, 55.8; H, 5.41; N, 0.0. Found: C, 55.4; H, 5.43; N, 0.22%.

*4.4.4. (R)-[trans-$(PEt_3)_2Pt(\mathbf{L})$]$_6$ (**4**)*

$^1H\{^{31}P\}$ NMR ($CDCl_3$): δ 7.84 (d, ^3J = 8.8 Hz, 12H), 7.77 (s, 12H), 7.34 (d, ^3J = 8.8 Hz, 12H), 7.18 (d, ^3J = 8.8 Hz, 12H), 6.99 (d, ^3J = 8.8 Hz, 12H), 2.19 (m, 72H), 1.87 (s, 36H), 1.23 (t, ^3J = 7.3 Hz, 108H). $^{31}P\{^1H\}$ NMR ($CDCl_3$): δ 12.47 ($^1J_{P-Pt}$ = 2366.3 Hz). $^{13}C\{^1H\}$ NMR ($CDCl_3$): δ 169.5, 146.0, 131.6, 131.1, 130.3, 128.9, 128.5, 126.1, 125.6, 123.3, 121.8, 109.6 (s, $^2J_{Pt-C}$ = 269.8 Hz), 109.26 (t, $^1J_{Pt-C}$ = 971.57 Hz, $^2J_{P-C}$ = 15.3 Hz), 20.6, 16.3 (t, $^1J_{P-C}$ = 17.4 Hz), 8.34. IR: ν(–C≡C–) 2089.5 cm^{-1} (m); ν(–C=O) 1762.4 cm^{-1} (s); MS (FAB): *m/z* 5088.2 (Calcd. *m/z* 5087.9 for $[M + H]^+$). Anal. Calc. for $C_{241}H_{278}Cl_2O_{24}P_{12}Pt_6 \cdot CH_2Cl_2$: C, 56.0; H, 5.42; N, 0.0. Found: C, 55.7; H, 5.06; N, 0.23%.

*4.4.5. (R)-[trans-$(PEt_3)_2Pt(\mathbf{L})$]$_7$ (**5**)*

$^1H\{^{31}P\}$ NMR ($CDCl_3$): δ 7.84 (d, ^3J = 8.8 Hz, 14H), 7.77 (s, 14H), 7.33 (d, ^3J = 8.8 Hz, 14H), 7.18 (d, ^3J = 8.8 Hz, 14H), 6.99 (d, ^3J = 8.8 Hz, 14H), 2.19 (m, 84H), 1.87 (s, 42H), 1.22 (t, ^3J = 7.3 Hz, 126H). $^{31}P\{^1H\}$ NMR ($CDCl_3$): δ 12.46 ($^1J_{P-Pt}$ = 2366.1 Hz). $^{13}C\{^1H\}$ NMR ($CDCl_3$): δ 169.4, 146.1, 131.6, 131.1, 130.4, 128.8, 128.5, 126.1, 125.7, 123.3, 121.8, 109.6 (s, $^2J_{Pt-C}$ = 267.5 Hz), 109.28 (t, $^1J_{Pt-C}$ = 972.1 Hz, $^2J_{P-C}$ = 14.8 Hz), 20.6, 16.4 (t, $^1J_{P-C}$ = 17.5 Hz), 8.33. IR: ν(–C≡C–) 2089.5 cm^{-1} (m); ν(–C=O) 1762.3 cm^{-1} (s). MALDI-TOF MS: *m/z* 5939.2 (Calcd. *m/z* 5935.7 for $[M + H]^+$). Anal. Calc. for $C_{280}H_{322}O_{28}P_{14}Pt_7$: C, 56.7; H, 5.47; N, 0.0. Found: C, 56.7; H, 5.39; N, 0.26%.

*4.4.6. (R)-[trans-$(PEt_3)_2Pt(\mathbf{L})$]$_8$ (**6**)*

$^1H\{^{31}P\}$ NMR ($CDCl_3$): δ 7.84 (d, ^3J = 8.8 Hz, 16H), 7.78 (s, 16H), 7.34 (d, ^3J = 8.8 Hz, 16H), 7.18 (d, ^3J = 8.8 Hz, 16H), 7.00 (d, ^3J = 8.8 Hz, 16H), 2.20 (m, 96H), 1.87 (s, 48H), 1.23 (t, ^3J = 7.3 Hz, 144H). $^{31}P\{^1H\}$ NMR ($CDCl_3$): δ 12.47 ($^1J_{P-Pt}$ = 2370.1 Hz). $^{13}C\{^1H\}$ NMR ($CDCl_3$): δ 169.4, 146.1, 131.7, 131.1, 130.4, 128.8, 128.5, 126.2, 125.7, 123.3, 121.8, 109.6 (s, $^2J_{Pt-C}$ = 266.9 Hz), 109.28 (t, $^1J_{Pt-C}$ = 968.6 Hz, $^2J_{P-C}$ = 14.3 Hz), 20.6, 16.4 (t, $^1J_{P-C}$ = 17.5 Hz), 8.34. IR: ν(–C≡C–) 2091.2 cm^{-1} (m); ν(–C=O) 1762.6 cm^{-1} (s). MALDI-TOF MS: *m/z* 6787.1 (Calcd. *m/z* 6782.5 for $[M + H]^+$). Anal. Calc. for $C_{332}H_{396}O_{32}P_{16}Pt_8 \cdot 2$hexane: C, 57.3; H, 5.74; N, 0.0. Found: C, 57.6; H, 5.71; N, 0.56%.

*4.5. Synthesis of **2a***

A mixture of **2** (9 mg, 2.65 μmol) and K_2CO_3 (5 mg) in methanol (2 mL) and THF (2 mL) were stirred at room temperature for 12 h. After the removal of all the volatiles, the residue was purified by silica-gel column chromatography (hexanes/ethyl acetate/dichloromethane: 1/1/1 v/v/v) to give **2a** in quantitative yield (8.1 mg). $^1H\{^{31}P\}$ NMR ($CDCl_3$): δ 7.83 (d, ^3J = 8.8 Hz, 8H), 7.73 (s, 8H), 7.30 (d, ^3J = 8.8 Hz, 8H), 7.18 (dd, ^3J = 8.8 Hz, ^4J = 8.8 Hz, 8H), 6.88 (d, ^3J = 8.8 Hz, 8H), 5.05 (s, 8H, –OH), 2.17 (q, ^3J = 7.3 Hz, 48H), 1.21 (t, ^3J = 7.3 Hz, 72H). $^{31}P\{^1H\}$ NMR ($CDCl_3$): δ 12.4 ($^1J_{Pt-P}$ = 2374.0 Hz). $^{13}C\{^1H\}$ NMR ($CDCl_3$): δ 152.0, 131.5, 131.1, 130.5, 129.5, 128.9, 124.5, 124.0, 117.7, 111.2, 109.6 (s, $^2J_{Pt-C}$ = 267.6 Hz), 108.26 (t, $^1J_{Pt-C}$ = 953.1 Hz, $^2J_{P-C}$ = 14.5 Hz), 16.44 (t, $^1J_{P-C}$ = 17.6 Hz), 8.32. MS (MALDI-TOF) *m/z* $[M + H]^+$ 3056.3 (Calcd. *m/z* 3056.0), $[M + Na]^+$ 3077.8 (Calcd. *m/z* 3078.0), $[M + K]^+$ 3094.9 (Calcd. *m/z* 3094.1).

*4.6. Synthesis of **2b***

Compound **2a** (46.5 mg, 0.015 mmol) and 1-bromododecane (57.9 mg, 0.1667 mmol) were added to a mixture of K_2CO_3 (64 mg), 18-crown-6 (1 mg) and THF (5 mL). The resulting mixture was heated to reflux for 3 days. Upon cooling to room temperature, the organic volatiles were removed and the residue was extracted with dichloromethane and washed with water. Pure **2b** was obtained by silica-gel column chromatography

(hexanes/ethyl acetate/dichloromethane: 15/1/1 v/v/v). Yield: 39 mg (50%). $^1H\{^{31}P\}$ NMR ($CDCl_3$): δ 7.77 (d, ^3J = 9.3 Hz, 8H), 7.70 (s, 8H), 7.32 (d, ^3J = 8.8 Hz, 8H), 7.09 (d, ^3J = 9.3 Hz, 8H), 6.89 (d, ^3J = 8.8 Hz, 8H), 3.90 (m, 16H, –OCH_2–), 2.18 (q, ^3J = 7.3 Hz, 48H), 1.42 (m, 16H), 1.27 (s, 176H, –$(CH_2)_{11}$–), 1.21 (t, ^3J = 7.8 Hz, 72H), 1.16 (m, 16H), 1.06 (m, 48H, –$(CH_2)_3$–), 0.89 (t, 24H, –CH_3). $^{31}P\{^1H\}$ NMR ($CDCl_3$): δ 12.35 ($^1J_{P-Pt}$ = 2378.8 Hz). MS (MALDI-TOF) *m/z* M^+ 5074.3 (Calcd. *m/z* 5074.8), $[M + Na]^+$ 5098.1 (Calcd. *m/z* 5097.8), $[M + K]^+$ 5113.3 (Calcd. *m/z* 5113.8).

4.7. Synthesis of **2c**

Compound **2a** (9.9 mg, 3.24 μmol) and G_1Br (15.6 mg, 0.31 mmol) were added to a mixture of K_2CO_3 (5 mg), 18-crown-6 (1 mg) and acetone (4 mL). The resulting mixture was heated to reflux for 3 days. Upon cooling to room temperature, the organic volatiles were removed and the residue was extracted with dichloromethane and washed with water. Pure **2b** was obtained by silica-gel column chromatography (hexanes/ethyl acetate/dichloromethane: 2/1/1 v/v/v). Yield: 9 mg (40%). $^1H\{^{31}P\}$ NMR ($CDCl_3$): δ 7.75 (d, ^3J = 9.3 Hz, 8H), 7.68 (s, 8H), 7.36 (d, ^3J = 9.3 Hz, 8H), 7.11 (d, ^3J = 9.3 Hz, 8H), 6.95 (d, ^3J = 8.8 Hz, 8H), 6.49 (d, ^4J = 1.96 Hz, 32H), 6.39 (t, ^4J = 2.22 Hz, 16H), 6.35 (t, ^4J = 2.22 Hz, 8H), 6.27 (t, ^4J = 1.47 Hz, 8H), 4.95 (m, 16H), 4.60 (s, 24H), 3.77 (s, 96H), 2.12 (q, ^3J = 7.8 Hz, 48H), 1.16 (t, ^3J = 7.8 Hz, 72H). $^{31}P\{^1H\}$ NMR ($CDCl_3$): δ 12.3 ($^1J_{P-Pt}$ = 2374.1 Hz). MS (MALDI-TOF) *m/z* M^+ 6434.5 (Calcd. *m/z* 6434.7), $[M + K]^+$ 6474.3 (Calcd. *m/z* 6473.8).

Appendix A. Supplementary data

Crystallographic data for the structural analysis have been deposited with the Cambridge Crystallographic Data Centre, CCDC No. 262940. Copies of this information may be obtained free of charge from The Director, CCDC, 12 Union Road, Cambridge CB2 1EZ, UK (fax: +44 1223 336 033; e-mail: deposit@ccdc.cam.ac.uk or www: http://www.ccdc.cam.ac.uk). Supplementary data associated with this article can be found, in the online version at doi:10.1016/j.jorganchem.2005.03.049.

References

[1] J.-M. Lehn, Supramolecular Chemistry: Concepts and Perspectives, VCH, New York, 1995.
[2] M. Fujita, Chem. Soc. Rev. 27 (1998) 417.
[3] K. Onitsuka, S. Yamamoto, S. Takahashi, Angew. Chem., Int. Ed. 38 (1999) 174.
[4] P.J. Stang, B. Olenyuk, Acc. Chem. Res. 30 (1997) 502.
[5] S. Leininger, B. Olenyuk, P.J. Stang, Chem. Rev. 100 (2000) 853.
[6] B.J. Holliday, C.A. Mirkin, Angew. Chem., Int. Ed. 40 (2001) 2022.
[7] P.H. Dinolfo, J.T. Hupp, Chem. Mater. 13 (2001) 3113.
[8] P.J. Stang, N.E. Persky, J. Manna, J. Am. Chem. Soc. 119 (1997) 4777.
[9] R.W. Saalfrank, I. Bernt, E. Uller, F. Hampel, Angew. Chem., Int. Ed. 36 (1997) 2482.
[10] G.R. Newkome, T.J. Cho, C.N. Moorefield, G.R. Baker, R. Cush, P.S. Russo, Angew. Chem., Int. Ed. 38 (1999) 3717.
[11] N. Matsumoto, Y. Motoda, T. Matsuo, T. Nakashima, N. Re, F. Dahan, J.P. Tuchagues, Inorg. Chem. 38 (1999) 1165.
[12] O. Mamula, A. von Zelewsky, G. Bernardinelli, Angew. Chem., Int. Ed. 37 (1998) 290.
[13] S.W. Lai, K.K. Cheung, M.C.W. Chan, C.M. Che, Angew. Chem., Int. Ed. 37 (1998) 182.
[14] B. Hasenknopf, J.-M. Lehn, N. Boumediene, A. DupontGervais, A. VanDorsselaer, B. Kneisel, D. Fenske, J. Am. Chem. Soc. 119 (1997) 10956.
[15] M.M. Ali, F.M. MacDonnell, J. Am. Chem. Soc. 122 (2000) 11527.
[16] B. Hasenknopf, J.-M. Lehn, J.B.O. Kneisel, G. Baum, D. Fenske, Angew. Chem., Int. Ed. 35 (1996) 1838.
[17] B. Grossmann, J. Heinze, E. Herdtweck, F.H. Kohler, H. Noth, H. Schwenk, M. Spiegler, W. Wachter, B. Weber, Angew. Chem., Int. Ed. 36 (1997) 387.
[18] P.L. Jones, K.J. Byrom, J.C. Jeffery, J.A. McCleverty, M.D. Ward, Chem. Commun. (1997) 1361.
[19] M. Laskoski, J.G.M. Morton, M.D. Smith, U.H.F. Bunz, Chem. Commun. (2003) 1628.
[20] P.-H. Ge, W. Fu, W.A. Herrmann, E. Herdtweck, C. Campana, R.A. Adams, U.H.F. Bunz, Angew. Chem., Int. Ed. 39 (2000) 387.
[21] D. Zhao, J.S. Moore, Chem. Commun. (2003) 807.
[22] J.S. Moore, Acc. Chem. Res. 30 (1997) 402.
[23] A.J. Gallant, M.J. MacLachlan, Angew. Chem., Int. Ed. 42 (2003) 5307.
[24] N.J. Long, C.K. Williams, Angew. Chem., Int. Ed. 42 (2003) 2586.
[25] H. Jiao, K. Costuas, J.A. Gladysz, J.-F. Halet, M. Guillemot, L. Toupet, F. Paul, C. Lapinte, J. Am. Chem. Soc. 125 (2003) 9511.
[26] W.-Y. Wong, G.-L. Lu, K.-H. Choi, J. Organomet. Chem. 659 (2002) 107.
[27] M.S. Khan, M.K. Al-Suti, M.R.A. Al-Mandhary, B. Ahrens, J.K. Bjernemose, M.F. Mahon, L. Male, P.R. Raithby, R.H. Friend, A. Koehler, J.S. Wilson, Dalton Trans. (2003) 65.
[28] S.J. Lee, A. Hu, W. Lin, J. Am. Chem. Soc. 124 (2002) 12948.
[29] S.J. Lee, W. Lin, J. Am. Chem. Soc. 124 (2002) 4554.
[30] H. Jiang, A. Hu, W. Lin, Chem. Commun. (2003) 96.
[31] L. Zhang, Y.-H. Niu, A.K.-Y. Jen, W. Lin, Chem. Commun. (2005).
[32] H. Jiang, W. Lin, J. Am. Chem. Soc. 126 (2004) 7426.
[33] Part of this paper has been previously communicated. See: H. Jiang, W. Lin, J. Am. Chem. Soc. 125 (2003) 8084.
[34] K. Onitsuka, Y. Harada, F. Takei, S. Takahashi, Chem. Commun. (1998) 643.
[35] V.W.W. Yam, Acc. Chem. Res. 35 (2002) 555.
[36] J. Chatt, B.L. Shaw, J. Chem. Soc. (1960) 4020.